

GENE EXPRESSION PROFILE OF HUMAN COLON CANCER CELLS TREATED WITH CROSS-REACTING MATERIAL 197, A DIPHTHERIA TOXIN NON-TOXIC MUTANT

S. RIVETTI^{1,2}, M. LAURIOLA^{1,2}, M. VOLTATTORNI³, M. BIANCHINI⁴, D. MARTINI⁵,
C. CECCARELLI⁶, A. PALMIERI⁷, G. MATTEI^{1,2}, M. FRANCHI⁵, G. UGOLINI⁸,
G. ROSATI⁸, I. MONTRONI⁸, M. TAFFURELLI⁸ and R. SOLMI^{1,2}

¹Dipartimento di Istologia, Embriologia e Biologia Applicata, Università di Bologna, Bologna; ²Centro di Ricerca in Genetica Molecolare "Fondazione CARISBO", Bologna; ³Laboratori di Biotecnologie, Università di Bologna, Bologna; ⁴Centro de Investigaciones Oncologicas (CIO-FUCA), Buenos Aires, Argentina; ⁵Dipartimento di Scienze Anatomiche Umane e Fisiopatologia dell'Apparato Locomotore Università di Bologna, Bologna; ⁶Dipartimento Clinico di Scienze Radiologiche e Istocitopatologiche, Università di Bologna, Bologna; ⁷D.M.C.C.C. Sezione di Chirurgia Maxillo-Facciale, Università di Ferrara, Ferrara; ⁸Dipartimento Emergenza/Urgenza, Chirurgia Generale e dei Trapianti, Università di Bologna, Bologna, Italy

Received February 15, 2011 – Accepted June 6, 2011

Cross-Reacting Material 197 (CRM197) is a diphtheria toxin non-toxic mutant that has shown anti-tumor activity in mice and humans. It is still unclear whether this anti-tumorigenic effect depends on its strong inflammatory-immunological property, its ability to inhibit heparin-binding epidermal growth factor (HB-EGF), or even its possible weak toxicity. CRM197 is utilized as a specific inhibitor of HB-EGF that competes for the epidermal growth factor receptor (EGFR), overexpressed in colorectal cancer and implicated in its progression. In this study we evaluate the effects of CRM197 on HT-29 human colon cancer cell line behaviour and, for CRM197 recognized ability to inhibit HB-EGF, its possible influence on EGFR activation. In particular, while HT-29 does not show any reduction of viability after CRM197 treatment (MTT modified assay), or changes in cell cycle distribution (flow cytometry), in EGFR localization, phospho-EGFR detected signals (immunohistochemistry) or in morphology (scanning electron microscopy, SEM) they show a change in the gene expression profile by microarray analysis (cDNA microarray SS-H19k8). The overexpression of genes like protein phosphatase 2, catalytic subunit, alpha isozyme (PPP2CA), guanine nucleotide-binding protein G subunit alpha-1 (GNAI1) and butyrophilin, subfamily 2, member A1 (BTN2A1) has been confirmed with real-time-qPCR. This is the first study where the CRM197 treatment on HT-29 shows a possible scarce implication of endogenous HB-EGF on EGFR expression and cancer cell development. At the same time, our results show the alteration of a specific and selected number of genes.

Diphtheria toxin (DT) has antitumor activity in mice (1) and in humans (2). First, its powerful toxicity was believed to provoke an anti-proliferative effect

against cancer. Subsequently, its strong inflammatory-immunological property was pointed out *in vivo* for achieving important antitumor results (3).

Key words: CRM197, colon cancer, microarray

Mailing address: Dr Rossella Solmi,
Dipartimento di Istologia,
Embriologia e Biologia Applicata,
Via Belmeloro, 8 40126 Bologna, Italy
Tel: ++39 051 2094100/2094109
Fax: ++39 051 2094110
e-mail: rossella.solmi@unibo.it

0394-6320 (2011)

Copyright © by BIOLIFE, s.a.s.

This publication and/or article is for individual use only and may not be further reproduced without written permission from the copyright holder. Unauthorized reproduction may result in financial and other penalties

In the early 1970s the virtually not-toxic mutant CRM197, was obtained from strains of *Corynebacterium diphtheriae* lysogenized with β -phages, owing to a single glycine to glutamic acid change in position 52. Although DT mutant CRM197 (Mr 58,422) is enzymatically inactive because of its inability to bind to NAD⁺ (4), it maintains the same immunological properties (3) and the ability to bind to the specific cell-membrane receptor of the native molecule. DT receptor (DTR) is the membrane-anchored form of HB-EGF (proHB-EGF) (5). The proHB-EGF (20-30 kD) contains an extracellular EGF-like domain, a transmembrane segment, and a short cytoplasmic tail (6). It is cleaved at the juxtamembrane domain via metalloprotease activation using a mechanism known as "ectodomain shedding", yielding a soluble EGF receptor ligand (HB-EGF) and a C-terminal fragment (CTF) containing transmembrane and cytoplasmic segments (HB-EGF-CTF) (7). CRM197 binds to DTR/proHB-EGF and HB-EGF at a very high affinity (8). HB-EGF competes for EGFR (6) and also binds ErbB4 (7). It is a potent mitogen and chemotactic factor (7) and it functions as an autocrine or paracrine factor (9-10). Increased HB-EGF expression, compared with normal tissues, was reported in colon (11), and in other different cancers (7). CRM197 inhibits the mitogenic action of HB-EGF by blocking its binding to ErbB receptors (5) without any influence on the other EGFR ligands and it sometimes exhibits a weak toxicity (8, 12-13). Few studies considered CRM197 effects on colorectal cancer (14). CRM197 is known to be the best specific inhibitor of HB-EGF. A ligand of EGFR could be an advantageous target for colorectal cancer therapy instead of EGFR for which, to date, there are many anti-EGFR agents with a controversial effectiveness. We chose to treat with CRM197, one of the most studied human colon cancer cell lines, the HT-29 that expresses endogenous levels of HB-EGF similar to the others frequently considered (15), to demonstrate, as a first approach, the possible influence of endogenous HB-EGF in cancer enterocytes *in vitro*. This cell line is positive to EGFR (16), but it is negative to ErbB4 (17).

MATERIALS AND METHODS

Compounds

CRM197, [Glu52]-Diphtheria toxin, from *Corynebacterium diphtheriae*, purchased from SIGMA

Saint Louis, Missouri, USA, was used for *in vitro* assays at the concentration of 1 μ g/ml.

Cell Line

HT-29 is a cell line isolated from a primary colon adenocarcinoma in a 44 year-old Caucasian female (60th to 65th passage) that was purchased from American Type Culture Collection (ATCC) and cultured in Dulbecco's minimal essential medium (DMEM), 25 mM glucose supplemented with 2 mM L-glutamine, antibiotics (100 U.mL⁻¹ penicillin and 100 mg.mL⁻¹ streptomycin) and with 10% (v/v) heat-inactivated fetal bovine serum (Cambrex, Verviers, Belgium). Cells were grown in a 37°C and 5% CO₂ air incubator. For all experiments the cells were treated when 70-80% confluent.

Cell-viability assay

Cell growth was determined using a variation on the MTT [3-(4,5-dimethylthiazol-2-yl)-2,5-diphenyl tetrazolium bromide] assay described by Mosmann (18). HT-29 cells were counted using Trypan Blue solution 10% in a Neubauer cell counter chamber (Brand, Wertheim, Germany) and observing viable (non-stained) and non-viable (stained) cells under a microscope (19). Cells were seeded into 25 cm² tissue culture flasks (Becton Dickinson Labware Europe Le Pont De Claix, France) at a concentration of 4.0 x 10⁵ cells per flask and incubated for 24 h at 37°C. After that, CRM197 was added and the flasks were incubated for 24, 48, 72 and 96 h, respectively. In order to establish the initial number of cells treated, extra flasks of HT-29 cells were treated with trypsin and then cells were counted. After drug incubation, cells were washed once with Phosphate Buffer Saline (PBS), harvested in 0.1% trypsin-1 mmol/L EDTA in PBS, and counted. Three independent experiments and three replicates for untreated and treated cells, respectively, were carried out.

Cell-cycle analysis

Cell-cycle analysis was performed by flow cytometry. HT-29 cells were cultured for 5 days then treated for 24 and 48 hours with CRM197. After detachment, they were washed twice with PBS and then resuspended in a solution containing 0.1% sodium citrate, 0.1% Nonidet 40, 50 μ g/mL propidium iodide and 10 μ g/mL RNAase. Cells were incubated for 30 min at 37°C in the dark.

The cell cycle profiles were determined using a Beckman Coulter Epics XL MCL Cytometer and analyzed by Modfit 5.0 software (20). Three independent experiments and three replicates were conducted for untreated and treated cells, respectively.

Immunohistochemistry

HT-29 cells were seeded into BD Falcon (BD, Franklin

Lakes, NJ USA) chamber glass slides at a concentration of 4×10^4 cells per chamber, incubated for 5 days, and then treated for 24 h with CRM197. They were fixed in cold methanol for 10 min at -20°C and dried for 3-5 min under laminar flow and then kept at -20°C until staining. Immunohistochemistry was performed using a non-biotin amplified method (Novolink, Novocastra Laboratories, Newcastle, UK).

Slides were thawed for 1 min at room temperature (RT) and immersed in a 0.5% methanol/ H_2O_2 solution for 10 min to abolish endogenous peroxidase activity, washed 3 times in distilled water and immersed in a PBS pH 7.2-7.4 solution for 10 min. Cells were incubated overnight at RT in a humidified atmosphere using an anti-EGFR monoclonal antibody (clone 31G7, Zymed Laboratories, San Francisco, CA, USA) diluted 1:120 and an anti-phosphoTyr1173 EGFR monoclonal antibody (Cell Signaling Tech., MA, USA) diluted 1:100. Cells were washed in PBS and processed using the Novolink system according to the manufacturer's suggested procedure. The reaction was developed using a 3-3'-diaminobenzidine tetrahydrochloride 50 mg/100 ml PBS solution activated with hydrogen peroxide for 10 min. Cell nuclei were counterstained using Mayer's Hematoxylin, dehydrated to xylene and mounted with BioMount (Bio-Optica, Milan, Italy). Two independent experiments and two replicates for untreated and treated cells were conducted per experiment.

Scanning electron microscopy (SEM)

HT-29 cells were seeded onto Lab-Tek four chamber permanox slides (Nunc, Naperville, IL, USA) at a concentration of 4×10^4 cells per chamber and incubated for 5 days. Cells were then treated for 24 h with CRM197. Two independent experiments and two replicates for untreated and treated cells were conducted per experiment. SEM (Philips SEM 515, Eindhoven, The Netherlands) was performed to examine the cell morphology. All the slides were delicately rinsed with PBS in order not to detach cells from the surfaces, then fixed with Karnovsky solution (1.5% glutaraldehyde, 1% paraformaldehyde, 0.1 M Cacodilate buffer) for 30 min. The slides with adhering cells were rinsed three times with Cacodilate buffer 0.1 M, postfixed for 30 min with Os_2O_4 1% in Cacodilate buffer, dehydrated with ethanol and finally dried with 2x hexamethyldisilazane (HDMS) for 15 min.

The slides were mounted on stubs with carbon bi-adhesive film, covered with a 20 nm-thick gold-palladium film and observed at 15 kV.

RNA extraction, real-time-qPCR and hybridization on cDNA arrays

HT-29 were cultured for 5 days, then treated for 24

h with CRM197. Then TRIzol (Invitrogen, Carlsbad, CA, USA) was used for RNA extraction, according to the manufacturer's protocol. For quantitative Real-Time RT-PCR, cDNA was synthesised using the SuperScriptII first-strand synthesis kit (Invitrogen, Carlsbad, CA). One microgram of RNA was reverse transcribed into cDNA with random primers (High Capacity cDNA Archive Kit, Applied Biosystems, Foster City, CA, USA). Real-time-qPCR analysis was performed using Power-SYBR Green (ABI, Carlsbad, CA). All experiments were carried out in triplicates, and results normalized to Beta-2-microglobulin (B2M) RNA levels. RT-qPCR primers: PPP2CA forward TGCCTTGGTGGATGGGCAGATCT and reverse ACCAACGTGAGGCCATTGGCA; GNAI1 forward GTGCTTGGAGCCCGCACTCGG and reverse AGATTCACCAGCACCGAGCAGCA; BTN2A1 forward TAGTGCCTGTGCCCCCTGGGC and reverse CCCCACGACAATAAACTGGGCTTC; Septin-6 (Sept-6) forward CTTGGTCGCGCCCGAAGTGT and reverse CCTTCACCCACCTGGCGAGC; B2M forward GGCATTCCTGAAGCTGAC and reverse TCTTTGGAGTACGCTGGATAG. Relative Gene Expression (RGE) was calculated with the 2-ddCt method (21). We analyzed differential gene expression using hybridization of SS-H19k8, representing 19,200 human cDNA clones (UHN, Microarray Centre, Toronto, ON, Canada). Ten micrograms of total RNA were used for each sample. cDNA was synthesized using a CyScribe Post-Labeling Kit (Amersham Biosciences Europe, Freiburg, Germany) that provides reagents for preparation of Cy3 and Cy5 labeled cDNA probes according to the manufacturer's protocol. Identical amounts of labelled cDNA from untreated and treated cells were mixed in DIG Easy hybridization solution and hybridized at 37°C overnight. Untreated HT-29 cDNA was labeled with Cy3 and CRM197-treated HT-29 cDNA was labeled with Cy5. Washing was performed twice for 10 min with 1 x saline sodium citrate (SSC), 0.1% sodium dodecyl sulfate (SDS) at 42°C , eight times for 5 min with 1 x SSC at room temperature and four times with 0.1 x SSC at room temperature. Slides were dried by centrifugation for 2 min at 2,000 rpm.

Microarray scanning and data analysis

Two biological microarray replicates were scanned using the GenePix 4000b microarray scanner (Axon, Molecular Devices, Union City, CA, USA); only DNA spots present in at least 66 % of the replicates were selected for analysis, signal intensities of Cy3 and Cy5 from the 20,000 spots were quantified and analyzed by substituting backgrounds, using GenePix Pro v6.1 software (Axon, Molecular Devices). The laser power for scanning green and red colours was adjusted in order

to obtain a global intensity ratio near to 1. If necessary, further washes were performed to reduce the background. Each spot was defined using the .gal file provided by the manufacturer, with automatic adjustment for the positioning of spot features. Spots showing no signal or obvious defects were flagged accordingly by visual inspection and excluded from the analysis.

Microarray data set was sorted and loaded on ExpressConverter v2.1, which enabled us to transform GenePix generated result files into the correct file format (.mev) to be properly used with MIDAS v2.19 (Microarray Data Analysis System). MIDAS was used to preprocess and normalize (within-slide LOWESS normalization) the raw microarray data. Moreover, it creates an output that could be easily loaded on Excel to automate the process of ratio calculation for each gene. Using the \log_2 ratios of selected genes, the reference list was generated by ranking the genes. To select genes with different expression we considered up-regulated genes as those with $\log_2 \text{Cy5/Cy3} > 1$ and down-regulated genes as those with $\log_2 \text{Cy5/Cy3} < -1$. The arrays were centered on median, and an unsupervised hierarchical clustering method with a correlation distance between two samples was performed (22).

RESULTS

Cell-viability by an MTT assay with Trypan blue solution

We tested 0.5, 1, 5 and 10 $\mu\text{g/ml}$ CRM197 concentrations (data not shown) and according to literature, we chose 1 $\mu\text{g/ml}$ for our biological priority. Kageyama (8) tested the drug efficacy at various concentrations on Vero cells. 1 $\mu\text{g/ml}$ and 10 $\mu\text{g/ml}$ resulted the best. To obtain the gene expression profile and the cell viability at 96 hours of treatment we decided to use 1 $\mu\text{g/ml}$. Moreover, a number of authors (23-24) used the same concentration for different cell types. HT-29 cells showed no statistically significant differences in cell viability between untreated and treated groups (Fig. 1).

Cell-cycle analysis by flow cytometry with propidium iodide

Flow cytometry analysis was performed to determine the influence of treatments on the HT-29 cell cycle (Fig. 2). Analysis with propidium iodide incorporation at 24 and 48 hours after the treatment with CRM197 showed no statistically significant differences between treated and untreated cells.

In fact the distribution of cells in the 3 phases of the cell cycle remained unchanged, with a preponderance of cells in G0/G1 and S phases.

Immunohistochemistry

EGFR expression and localization

After treatment with CRM197, the EGFR (Fig. 3 a, b) and phospho-EGFR (Fig. 3 c, d) immunostaining did not show differences between untreated (Fig. 3, a and c, respectively) and treated HT-29 cells (Fig. 3, b and d, respectively). No EGFR and phospho-EGFR modifications were highlighted. Moreover, the quote of phospho-EGFR signal on the total remained unchanged, underlining no direct influence on the EGFR receptor.

SEM

Ultrastructure phenotype on surface morphology in CRM197 treatment

HT-29 cells treated with CRM197 did not show any morphological differences in the ultrastructure, when compared with untreated cells. In fact, they showed the same microvilli distribution, the same cellular contacts and every other morphological feature was also conserved (Fig. 4).

DNA microarray data analysis

CRM197 effect on global gene expression profile

HT-29 cell line responded to CRM197 treatment with changes in gene expression, as revealed by cDNA microarray profiling (Fig. 5). CRM197 treatment significantly up-regulated more than 2-fold 32 genes and down-regulated more than 2-fold 30 genes, as showed in Table I. Among the up-regulated genes, guanine nucleotide-binding protein G subunit alpha-1 (GNA11) and cholinergic receptor, muscarinic 1 (CHRM1) are G-related transducers in transmembrane signaling systems. Phosphorylase kinase, gamma 2 (PHKG2), F-box protein 3 (FBXO3) and protein phosphatase 2, catalytic subunit, alpha isozyme (PPP2CA) act on cell proliferation and differentiation. Butyrophilin, subfamily 2, member A1 (BTN2A1) encodes for an integral plasma membrane B box protein involved in lipid, fatty-acid and sterol metabolism. ARP1 actin-related protein 1 homolog A, centractin alpha (ACTR1A) and vacuolar protein sorting 41 (VPS41) are involved in vesicles trafficking in the Golgi

complex. Bloom syndrome, RecQ helicase-like (BLM) and cleavage and polyadenylation specific factor 3 (CPSF3) participate in DNA replication, repair and translation. Karyopherin alpha 4, importin alpha 3 (KPNA4) functions in nuclear protein import as an adapter protein for nuclear receptor KPNB1. Poly rC binding protein 1 (PCBP1) is a single-stranded nucleic acid binding protein that binds preferentially to oligo dC.

PAX interacting with transcription-activation domain protein 1 (PAXIP1) and zinc finger protein 415 (ZNF415) are involved in transcriptional regulation.

Among the down-regulated genes, SNW domain containing 1 (SNW1) is a splicing factor of pre-mRNA splicing. Zinc finger protein 486 (ZNF486), zinc finger and BTB domain containing 17 (ZBTB17) and activating transcription factor 7 interacting protein (ATF7IP) are involved in transcriptional regulation. Fibulin 5 (FBLN5) and fibronectin type III extracellular matrix proteins (FNDC4) promote adhesion. Retention in endoplasmic reticulum 1 (RER1), synaptotagmin-13 (SYT13) and WASH complex subunit 7 (KIAA1033) are involved in vesicles trafficking plasma membrane-Golgi complex. S100 calcium binding protein A6, calcyclin (S100A6), Septin-6 (Sept-6), Septin-7 (Sept-7), Septin-11 (Sept-11) and stathmin-2 (STMN2) are implicated in cytoskeleton reorganization. Proteasome subunit alpha type-2 (PSMA2), proteasome, prosome, macropain, 26S subunit, ATPase, 3 (PSMC3), ubiquitin-like modifier activating enzyme 6 (UBA6) and F-box protein 30 (FBXO30) are related to ubiquitin and ATP-dependent protein rearrangement. NAD synthetase, EC 6.3.5.1 (NADSYN1), Ubiquinone, also known as coenzyme Q (COQ3) and 3-hydroxy-3-methylglutaryl-Coenzyme A synthase 1 (HMGCS1) have a major role in the mitochondrial energetic process.

Real-Time-qPCR

mRNA expression in a subset of genes regulated by CRM197

The expression profiles of a group of genes identified by microarray to be induced by CRM197 treatment, like PPP2CA, BTN2A1, GNAI1 or downregulated like Sept-6 were analyzed by

quantitative real-time PCR. Validation of the patterns of these 4 genes by using RT-qPCR, confirmed gene expression activity of CRM197 in line with microarray results (Fig. 6). In detail the RT-qPCR results showed upregulation of PPP2A, GNAI1 and BTN2A1 in a range between 3.6 to 5-fold, in HT-29 cells treated with CRM197 compared to the untreated control condition.

DISCUSSION

EGFR is a pleiotropic signaling molecule (25). ErbB ligands are numerous and classified into four major groups, based on their direct binding to a particular ErbB family member. EGF, transforming growth factor-alpha and amphiregulin bind exclusively to EGFR (26). The second group includes HB-EGF, betacellulin and epiregulin, which bind to both EGFR and ErbB4. Neuregulin-1 (NRG-1) and NRG-2 bind to ErbB3 and ErbB4 and the fourth group include NRG-3 and NRG-4 that bind only ErbB4. No ligands bind directly to ErbB2, which forms heterodimers with other ErbB receptors and enhances the tyrosine kinase signals (7, 26). In colorectal cancer, EGFR is an important target for therapy, while no EGFR ligands are considered. There is a potential advantage in targeting an EGFR ligand compared to an ErbB receptor, as HB-EGF binds to EGFR and ErbB4, and eventually activates EGFR, ErbB2 and ErbB4. Our study, using CRM197, evaluated also the influence of the HB-EGF present in HT-29 on EGFR expression and colon cancer cell arrangement. Interestingly, the cell treatment with CRM197 changed the HT-29 gene expression profile and acted on a selected number of genes without interfering with the general cell behavior. Our HT-29 DNA microarrays showed a specific gene response to CRM197 treatment, but no direct effect on EGFR.

It has been shown that CRM197 is able to increase the dimensions of endosomes and inhibit their subsequent maturation (27). We observed up- and down-regulated genes in relation to endosome transformations by CRM197. We found up-regulated (ACTR1A, VPS41) and down-regulated (RER1, SYT13, KIAA1033) genes involved in vesicles trafficking plasma membrane-Golgi complex; genes implicated in cytoskeleton reorganization (S100A6, Sept-6, Sept-7, Sept-11, STMN2) and genes related to

Table I. Significantly regulated genes for HT-29 treated with CRM197.

Upregulated	
Gene Symbol	Gene Description
GNAI1	Guanine nucleotide-binding protein (G protein), alpha inhibiting activity polyp 110
CLCN4	Chloride channel 4
TGF-B	Transforming growth factor-beta activated kinase 1/MAP3K7 binding protein 2
BTN2A1	Butyrophilin, sub-family 2, member A1
SRGN	Secretory granule proteoglycan core precursor
PHKG2	Phosphorylase kinase, gamma 2 (testis)
PHF10	PHD finger protein 10
KPNA4	Karyopherin alpha 4 (importin alpha 3)
PPP2CA	Protein Phosphatase 2 (formerly 2A), catalytic subunit, alpha isoform
CCT3	Chaperonin containing TCP1, subunit 3 (gamma)
CD36	CD36 antigen (collagen type 1 receptor, thrombospondin receptor)
ACTR1A	ARP1 actin-related protein 1 homolog A, centractin alpha (yeast)
CHRM1	Cholinergic Receptor, Muscarinic 1
NMNAT2	Nicotinamide Nucleotide Adenylyltransferase 2
BLM	Bloom syndrome
CPSF3	Cleavage and polyadenylation specific factor 3, 73kDa
WHSC1	Wolf-Hirschhorn syndrome candidate 1
SCCPDH	Saccharopine dehydrogenase
ZNF415	Zinc finger protein 415
STX3	Syntaxin 3
KIAA1109	Hypothetical protein KIAA1109
PCBP1	Poly(rC) binding protein 1
PAXIP1	PAX interacting (with transcription-activation domain) protein 1
BDH1	3-hydroxybutyrate dehydrogenase, type 1
FBXO3	F-box only protein 3
CDNA FLJ46440	CDNA FLJ46440 fis, clone THYMU3016022
VPS41	Vacuolar Protein Sorting 41 (yeast)
KIAA0759	Hypothetical protein KIAA0759
MGC11266	Hypothetical protein MGC11266
EDEM1	ER degradation enhancer, mannosidase alpha-like 1
CDNA FLJ12187	CDNA FLJ12187 fis, clone MAMMA1000831
ELL3	Elongation factor, RNA polymerase II, 2
Downregulated	
Gene Symbol	Gene Description
CPSF7	Cleavage and polyadenylation specific factor 7, 59kDa
SFRS13A	Splicing factor, arginine/serine-rich
SEPT11	Septin 11
ZNF486	Zinc finger protein 486
ZBTB17	Zinc finger and BTB domain containing 17
HMGCS1	3-hydroxy-3-methylglutaryl-Coenzyme A synthase 1 (soluble)
ZNF117	Zinc finger protein 117
NADSYN1	NAD synthetase 1
KBTBD3	Kelch repeat and BTB (POZ) domain containing 3
S100A6	S100 calcium binding protein A6 (calcyclin)
SEPT7	Septin 7
FBLN5	Fibulin 5
STMN2	Stathmin-like 2
ATF7IP	Activating transcription factor 7 interacting protein
MGEA5	Meningioma expressed antigen 3 (yaluronidase)
MMP2	Matrix metalloproteinase 2 (gelatinase A, 72kDa type IV collagenase)
PSMA2	Proteasome (prosome, macropain) subunit, alpha type, 2
PEX19	Peroxisomal biogenesis factor 19

PSMC3	Proteasome (prosome, macropain) 26S subunit, ATPase, 3
KIAA1033	KIAA1033 protein
RER1	RER1 homolog (<i>S. cerevisiae</i>)
UBA6	Ubiquitin-like modifier activating enzyme 6
FNDC4	Fibronectin type III domain containing 4
COQ3	Coenzyme Q3 homolog, methyltransferase (yeast)
ADCY10	Adenylate cyclase 10 (soluble)
PRLR	Prolactin receptor
SYT13	Synaptotagmin XIII
SEPT6	Septin 6
FBXO30	F-box protein 30
SNW1	SNW domain containing 1

Genes were selected with p -values < 0.05 and a fold change above 2 (Upregulated) or below $\frac{1}{2}$ (Downregulated); $1 \mu\text{g/ml}$ CRM197 treatment.

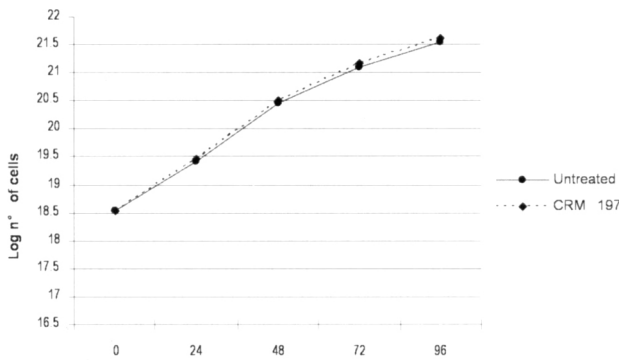


Fig. 1. HT-29 viability assay. Cells treated with $1 \mu\text{g/ml}$ of CRM197 between 0 and 96 hours. Each point represents a mean of triplicate values for each sample.

ubiquitin and ATP-dependent protein rearrangement (PSMA2, PSMC3, UBA6 and FOXO30).

In particular, we validated the overexpression of PPP2CA, GNAI1 and BTN2A1 genes. In previous studies on HT-29, PPP2CA results a starting point in pathways that lead to apoptosis, endoplasmatic reticulum (ER) stress-dependent (28) and MEK/ERK (29) pathways. GNAI1 is one of the guanine nucleotide-binding proteins (G proteins) involved as modulators or transducers in various transmembrane signaling systems. Specifically it is one of the G(i) proteins that are inhibitory GTP-binding regulators of adenylate cyclase (30). It is involved in MAPK/ERK signaling (<http://www.cellsignal.com/pathways/map-kinase.jsp>).

The BTN2A1 is a member of the BTN2

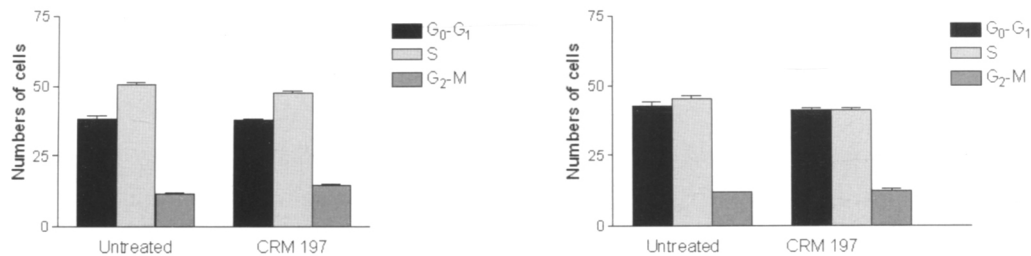


Fig. 2. Cell cycle distribution. Untreated and treated (CRM197) cells at 24 and 48 hours, respectively.

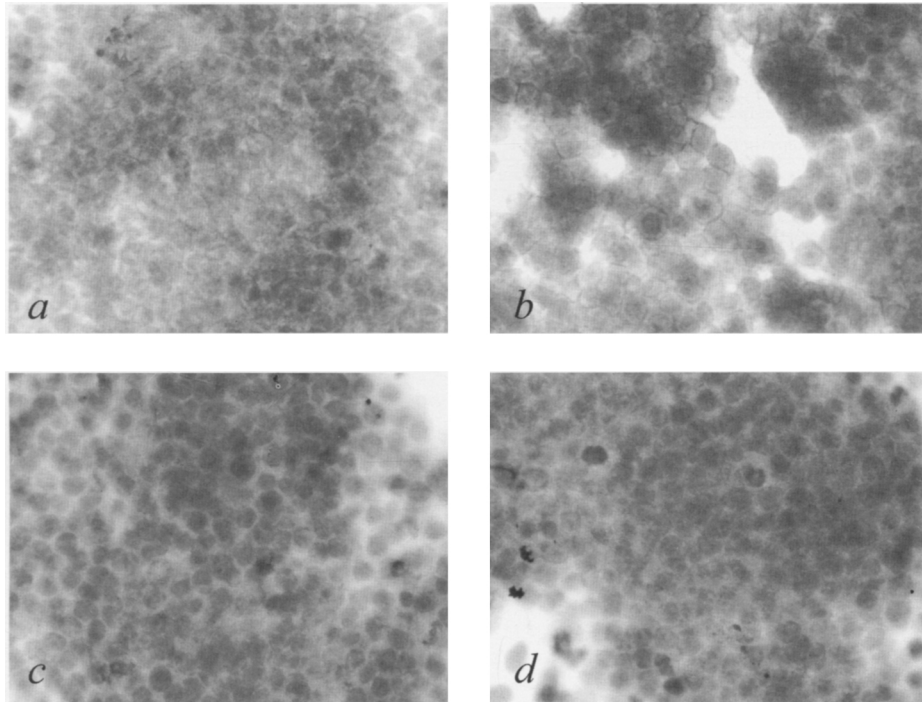


Fig. 3. HT-29 EGFR and phospho-EGFR immunostaining pattern. EGFR (**a**, **b**) and phospho-EGFR (**c**, **d**) in cells untreated and treated with CRM197, respectively. **a**, **b**. Continuous membrane staining is evident. **c**, **d**. Diffuse, granular cytoplasmic immunostaining is present.

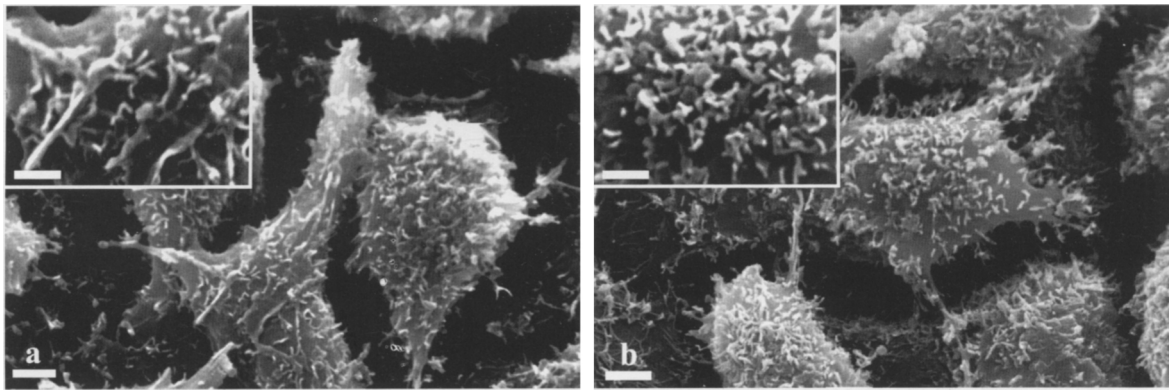


Fig. 4. HT-29 scanning electron microscopy. $\times 4000$ (bar $2 \mu\text{m}$). Evident cellular boundaries with filopodi and lamellipodi. Inserts: $\times 8000$ (bar $1 \mu\text{m}$). Short microvilli are present. **a**) Untreated cells. **b**) CRM197 treated cells.

subfamily of butyrophilins (BTN) belonging to the Ig superfamily, and it is encoded in a cluster of seven genes in the extended MHC class I region on chromosome 6 (31). BTN2A1 is an integral plasma membrane B-box protein that contributes to lipid, fatty acid, and sterol metabolism (Entrez Gene, NCBI). BTN2A1 mRNA is present in most human

tissues, including circulating immune cells. Many butyrophilin and butyrophilin-like proteins have been found to regulate immune function.

Even though in HT-29 the endogenous HB-EGF resulted poorly implicated in the overexpression of EGFR and in cancer behaviour, the gene expression changes shown in colon cancer cells after CRM197

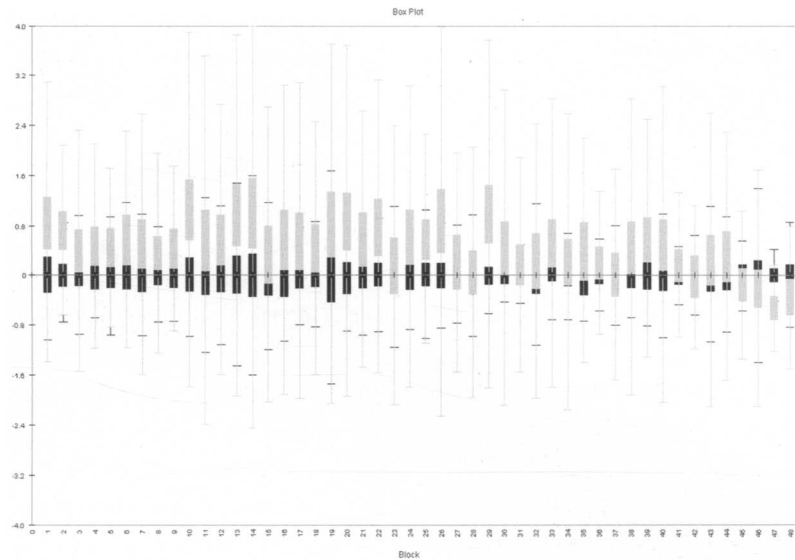


Fig. 5. Box graph. This graph depicts how the distribution of expression values ($\log_2 I(B)/I(A)$) of spots varies among different blocks within a slide, where $I(A)$ denotes the Cy5 (CRM197 treated cells) intensity of each spot in the slide and $I(B)$ denotes the Cy3 (untreated cells) intensity of each spot in the slide. This graph shows the effect of Locfit (LOWESS) normalization (gray bars pre-normalization, black bars, post-normalization).

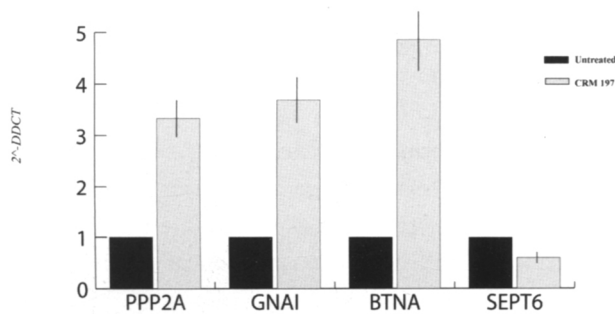


Fig. 6. Real-time-qPCR of a group of CRM197 affected genes in HT-29 colon cancer cells. HT-29 cells were treated for 24 hours with CRM197. To determine fold change, mRNA was isolated in CRM 197 treated and untreated conditions. All experiments were carried out in triplicates, and results normalized to Beta-2-microglobulin RNA levels. The fold was calculated as 2^{-DDCT} .

treatment, could influence a possible effectiveness of CRM197 *in vivo*, in presence of a more complex environment with the cancer stroma, surrounding stromal and inflammatory cells. More studies are necessary to better understand the comprehensive response to CRM197 *in vivo*. In effect, in 1991 Higashiyama (6), for the first time, showed that HB-EGF is expressed in macrophages and recent evidence (14, 32) underlined the elevated HB-EGF protein expression in the mucosa surrounding

colorectal adenocarcinomas, thus our *in vitro* data on HB-EGF in colon cancer cells are only a part of a complex system where HB-EGF acts, but they underline a set of selected genes involved in response to CRM197.

ACKNOWLEDGEMENTS

This study was supported by grants from the “Fondazione Enzo Piccinini” and “Fondazione Elio

Bisulli”.

The Authors thank Dr. Paolo Comeglio for the expert revision of the English language of the manuscript.

REFERENCES

- Buzzi S, Maistrello I. Inhibition of growth of Erlich tumors in Swiss mice by diphtheria toxin. *Cancer Res* 1973; 33:2349-53.
- Buzzi S. Diphtheria toxin treatment of human advanced cancer. *Cancer Res* 1982; 42:2054-8.
- Buzzi S, Rubboli D, Buzzi G, Buzzi AM, Morisi C, Pironi F. CRM197 (nontoxic diphtheria toxin): effects on advanced cancer patients. *Cancer Immunol Immunother* 2004; 53:1041-8.
- Giannini G, Rappuoli R, Ratti G. The amino-acid sequence of two non-toxic mutants of diphtheria toxin: CRM45 and CRM197. *Nucleic Acids Res* 1984; 12:4063-9.
- Mitamura T, Higashiyama S, Taniguchi N, Klagsbrun M, Mekada E. Diphtheria toxin binds to the epidermal growth factor (EGF)-like domain of human heparin-binding EGF-like growth factor/diphtheria toxin receptor and inhibits specifically its mitogenic activity. *J Biol Chem* 1995; 270:1015-9.
- Higashiyama S, Abraham JA, Miller J, Fiddes JC, Klagsbrun M. A heparin-binding growth factor secreted by macrophage-like cells that is related to EGF. *Science* 1991; 251:936-9.
- Miyamoto S, Yagi H, Yotsumoto F, Kawarabayashi T, Mekada E. Heparin-binding epidermal growth factor-like growth factor as a novel targeting molecule for cancer therapy. *Cancer Sci* 2006; 97:341-7.
- Kageyama T, Ohishi M, Miyamoto S, Mizushima H, Iwamoto R, Mekada E. Diphtheria toxin mutant CRM197 possesses weak EF2-ADP-ribosyl activity that potentiates its anti-tumorigenic activity. *J Biochem* 2007; 142:95-104.
- Hashimoto K, Higashiyama S, Asada H, et al. Heparin-binding epidermal growth factor-like growth factor is an autocrine growth factor for human keratinocytes. *J Biol Chem* 1994; 269:20060-6.
- Freeman MR, Yoo JJ, Raab G, Soker S, Adam RM, Schneck FX, Renshaw AA, Klagsbrun M, Atala A. Heparin-binding EGF-like growth factor is an autocrine growth factor for human urothelial cells and is synthesized by epithelial and smooth muscle cells in the human bladder. *J Clin Invest* 1997; 99:1028-36.
- Raab G, Klagsbrun M. Heparin-binding EGF-like growth factor. *Biochim Biophys Acta* 1997; 1333:179-99.
- Qiao J, Ghani K, Caruso M. Diphtheria toxin mutant CRM197 is an inhibitor of protein synthesis that induces cellular toxicity. *Toxicol* 2008; 51:473-7.
- Kimura Y, Saito M, Kimata Y, Kohno K. Transgenic mice expressing a fully nontoxic diphtheria toxin mutant, not CRM197 mutant, acquire immune tolerance against diphtheria toxin. *J Biochem* 2007; 142:105-12.
- Ichise T, Adachi S, Ohishi M, Ikawa M, Okabe M, Iwamoto R, Mekada E. Humanized gene replacement in mice reveals the contribution of cancer stroma-derived HB-EGF to tumor growth. *Cell Struct Funct* 2010; 35:3-13.
- Yotsumoto F, Yagi H, Suzuki SO, et al. Validation of HB-EGF and amphiregulin as targets for human cancer therapy. *Biochem Biophys Res Commun* 2008; 365:555-61.
- Solmi R, Lauriola M, Francesconi M, et al. Displayed correlation between gene expression profiles and submicroscopic alterations in response to cetuximab, gefitinib and EGF in human colon cancer cell lines. *BMC Cancer* 2008; 8:227.
- Yonezawa M, Wada K, Tatsuguchi A, et al. Heregulin-induced VEGF expression via the ErbB3 signaling pathway in colon cancer. *Digestion* 2009; 80:215-25.
- Mosmann T. Rapid colorimetric assay for cellular growth and survival: application to proliferation and cytotoxicity assays. *J Immunol Methods* 1983; 65:55-63.
- Freshney R. Culture of animal cells: a manual of basic technique. In *Technique*. Fogh J, ed. Plenum Press NY and London. New York 1987.
- Nusse M, Beisker W, Hoffmann C, Tarnok A. Flow cytometric analysis of G1- and G2/M-phase subpopulations in mammalian cell nuclei using side scatter and DNA content measurements. *Cytometry* 1990; 11:813-21.
- Livak KJ, Schmittgen TD. Analysis of relative gene

- expression data using real-time quantitative PCR and the 2(-Delta Delta C(T)) Method. *Methods* 2001; 25: 402-8.
22. Eisen MB, Spellman PT, Brown PO, Botstein D. Cluster analysis and display of genome-wide expression patterns. *Proc Natl Acad Sci USA* 1998; 95:14863-8.
 23. Pan B, Sengoku K, Goishi K, Takuma N, Yamashita T, Wada K, Ishikawa M. The soluble and membrane-anchored forms of heparin-binding epidermal growth factor-like growth factor appear to play opposing roles in the survival and apoptosis of human luteinized granulosa cells. *Mol Hum Reprod* 2002; 8:734-41.
 24. Yagi H, Yotsumoto F, Sonoda K, Kuroki M, Mekada E, Miyamoto S. Synergistic anti-tumor effect of paclitaxel with CRM197, an inhibitor of HB-EGF, in ovarian cancer. *Int J Cancer* 2009; 124:1429-39.
 25. Bauer-Mehren A, Furlong LI, Sanz F. Pathway databases and tools for their exploitation: benefits, current limitations and challenges. *Mol Syst Biol* 2009; 5:290.
 26. Rowinsky EK. The erbB family: targets for therapeutic development against cancer and therapeutic strategies using monoclonal antibodies and tyrosine kinase inhibitors. *Annu Rev Med* 2004; 55:433-57.
 27. Antignani A, Youle RJ. Endosome fusion induced by diphtheria toxin translocation domain. *Proc Natl Acad Sci USA* 2008; 105:8020-5.
 28. Guichard C, Pedruzzi E, Fay M, et al. Dihydroxyphenylethanol induces apoptosis by activating serine/threonine protein phosphatase PP2A and promotes the endoplasmic reticulum stress response in human colon carcinoma cells. *Carcinogenesis* 2006; 27:1812-27.
 29. Yu LG, Packman LC, Weldon M, Hamlett J, Rhodes JM. Protein phosphatase 2A, a negative regulator of the ERK signaling pathway, is activated by tyrosine phosphorylation of putative HLA class II-associated protein I (PHAPI)/pp32 in response to the antiproliferative lectin, jacalin. *J Biol Chem* 2004; 279:41377-83.
 30. Suki WN, Abramowitz J, Mattera R, Codina J, Birnbaumer L. The human genome encodes at least three non-allelic G proteins with alpha i-type subunits. *FEBS Lett* 1987; 220:187-92.
 31. Jeong J, Rao AU, Xu J, Ogg SL, Hathout Y, Fenselau C, Mather IH. The PRY/SPRY/B30.2 domain of butyrophilin 1A1 (BTN1A1) binds to xanthine oxidoreductase: implications for the function of BTN1A1 in the mammary gland and other tissues. *J Biol Chem* 2009; 284:22444-56.
 32. Clarke PA, Dickson JH, Harris JC, Grabowska A, Watson SA. Gastrin enhances the angiogenic potential of endothelial cells via modulation of heparin-binding epidermal-like growth factor. *Cancer Res* 2006; 66:3504-12.